Self-amplification of electrons emitted from surfaces in plasmas with E×B fields

2015 Plasma Sources Sci. Technol. 24 034010

(http://iopscience.iop.org/0963-0252/24/3/034010)

IOP Publishing Plasma Sources Science and Technology

Plasma Sources Sci. Technol. **24** (2015) 034010 (7pp) doi:10.1088/0963-0252/24/3/034010

Self-amplification of electrons emitted from surfaces in plasmas with E × B fields

M D Campanell[1,2], H Wang, I D Kaganovich and A V Khrabrov

Princeton Plasma Physics Laboratory, Princeton University, Princeton, New Jersey 08543, USA

E-mail: michaelcampanell@gmail.com

Received 31 January 2015, revised 2 April 2015
Accepted for publication 8 May 2015
Published 8 June 2015

Abstract

Emission from surfaces is known to cause enhanced wall heating and enhanced energy loss from plasma electrons. When E × B fields are present, emitted electrons are heated by the drift motion and cause enhanced transport along E. All emission effects are normally predicted to reach a maximum when the sheath becomes space-charge limited because any 'additional' emitted electrons return to the wall. But the returning electrons are also heated in the E × B drift, further enhancing transport, and return to the wall with extra energy, further enhancing the energy flux. Returning electrons can gain enough energy to induce secondaries, thereby self-amplifying to higher intensities. This newly analyzed mechanism could affect the wall heating, transport and global energy balance under certain conditions. Theory and simulations are presented.

Keywords: sheaths, electron emission, simulation

(Some figures may appear in colour only in the online journal)

1. Introduction

Electron emission from plasma-facing walls has several important consequences. Firstly, the sheath potential must change because more plasma electrons must reach the wall to maintain zero current. Sheath modification is essential to take into account to understand, for example, emissive probe measurements [1] and the interactions between emitting dust grains [2]. Secondly, emission enhances the wall heating because the extra plasma electrons that hit the wall are hotter than the emitted electrons leaving ($T_p >> T_{emit}$). This is critical in plasma devices including tokamaks [3], mirrors [4], and thrusters [5]. Thirdly, most magnetized plasmas have a nonzero electric field component **E** perpendicular to **B** [6, 7]. Emitted electrons entering the plasma move across **B** in the E × B drift, causing 'near wall conductivity' (NWC) [8]. NWC is a key mechanism of non-classical transport.

In the literature, all effects of emission are generally predicted to have certain limits. The flux of plasma electrons to a wall has a maximum possible value (the 'thermal flux') which depends on plasma density and temperature. The flow of emitted electrons entering the plasma cannot exceed the thermal flux either (zero current consideration). If the emitted flux *from the wall* exceeds the thermal flux, the sheath must change from the usual classical Debye sheath to either the space-charge limited (SCL) [9–11] or inverse [12, 13] sheath, see figure 1(a). In these two regimes, a potential barrier returns the 'surplus' electrons to the wall. When an emission barrier exists, the flows of electrons from the plasma into the wall (responsible for energy loss and wall heating), and from the wall into the plasma (responsible for NWC), are maximum. Therefore, it is normally assumed that the energy loss [14] and NWC [5, 15] cannot get larger even if the emission intensity gets larger. Any additional emitted electrons are assumed to return promptly to the wall without playing a role.

We will show that the returning electrons are significant under certain conditions. Because they do not return instantly, they have time to accelerate in the background **E** field, enhancing NWC, and return to the walls with extra energy, enhancing the wall heating and enhancing the energy loss from the system globally. These enhancements increase further if the returning electrons induce secondaries, which will undergo the same E × B heating and return to induce more secondaries, *etc*.

This paper will explore the physics of returning electrons and their 'self-amplification'. In section 2, we present a theoretical model estimating the extent of amplification in terms of a system's properties. A range of conditions with strong

[1] Author to whom any correspondence should be addressed.
[2] Currently at the Lawrence Livermore National Laboratory.

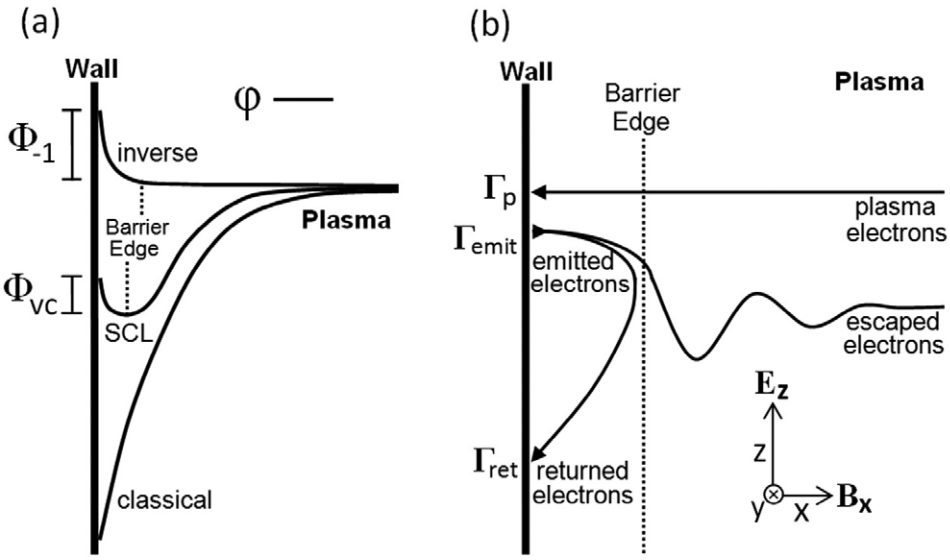

Figure 1. Qualitative sketch of the physics considered. (a) Possible potential distributions $\varphi(x)$ near plasma-facing surfaces that emit electrons. The SCL and inverse sheaths have potential barriers that return some electrons to the wall. (b) Averaged flows (the trajectory of the centroid in the x–z plane) of plasma electrons, escaped electrons and returned electrons in an E × B system with an emission barrier. The incoming plasma electrons have zero *average* motion across **B** because their E × B drifts are phase mixed. The emitted electrons start to drift quasi-coherently across **B**. Some escape the barrier; their average motion across **B** oscillates but damps with increasing x due to phase mixing [8]. The emitted electrons suppressed by the barrier return to the wall displaced along E_z. Having more energy than they started with, they may induce secondaries and thereby self-amplify.

amplification is predicted. In section 3, we study returning electrons in particle simulations and find that they can be the dominant mechanism of transport and energy flux when amplification is strong. We discuss implications in section 4 and give concluding remarks in section 5.

2. Theoretical analysis

2.1. Mathematical model

Consider a plasma contacting a floating wall, as diagrammed in figure 1. Let E_z and B_x represent the magnitudes of uniform crossed background fields. Bulk plasma electrons striking the wall produce an influx Γ_p. We denote γ_p as the average number of secondaries induced per plasma electron. When $\gamma_p > 1$, some secondaries must return to the wall, or else the ion flux cannot be balanced. Often it is assumed that the sheath is SCL [9–11]. The 'virtual cathode' Φ_{vc} is the potential barrier that suppresses the extra secondaries, figure 1(a). Recent theory and simulation works have also shown that strongly emitting sheaths can be positive, where ions are repelled from the wall [12, 13]. The 'inverse sheath' Φ_{-1} is a barrier to secondaries, acting in a similar way to a virtual cathode, see figure 1(a). Sheath structures are not measured in most experimental applications, so it is not yet known which sheath really forms at emitting surfaces. In both the SCL and inverse regimes, the dynamics of the returned secondaries would be similar. Our analytical treatment will model an inverse case, but the results as far as amplification is concerned would be the same even if the sheath were SCL.

Let Γ_{ret} denote the wall flux from returning electrons. If we now allow that returning electrons may induce secondaries at some average rate γ_{ret}, the floating condition at the wall becomes,

$$\Gamma_p(1-\gamma_p)+\Gamma_{ret}(1-\gamma_{ret})=\Gamma_{ion}. \quad (1)$$

Γ_p is the thermal flux of electrons from the plasma, generally known or calculable in terms of plasma properties. The γ_p is calculable in terms of the measured wall material emission yield and the plasma electron temperature [16]. The ion flux is small compared to Γ_p in an inverse sheath (or SCL) regime, so we can approximate $\Gamma_{ion} \approx 0$ [12]. Overall, Γ_{ret} can be calculated in terms of known system parameters and γ_{ret}. From equation (1),

$$\Gamma_{ret}=\frac{\Gamma_p(\gamma_p-1)}{1-\gamma_{ret}}. \quad (2)$$

We see that the returning flux is self-amplified by a factor $(1-\gamma_{ret})^{-1}$. The amplification factor becomes very large if γ_{ret} approaches unity. This is important because any energy flux and transport produced by returning secondaries is amplified by the same factor.

Amplification also changes the inverse sheath potential as follows. The total emitted flux induced by the plasma electrons and the returning electrons combined is,

$$\Gamma_{emit}=\gamma_p\Gamma_p+\gamma_{ret}\Gamma_{ret}. \quad (3)$$

All secondaries emitted with initial energies less than $q_e\Phi_{-1}$ will return to the wall (we will omit the '-1' subscript from now on for convenience). If the initial energy distribution of secondaries is an isotropic Maxwellian with temperature T_{emit}, then

$$\Gamma_{ret}=\left[1-\exp\left(\frac{-q_e\Phi}{T_{emit}}\right)\right]\Gamma_{emit}. \quad (4)$$

Combining equations (2)–(4) yields an expression for Φ,

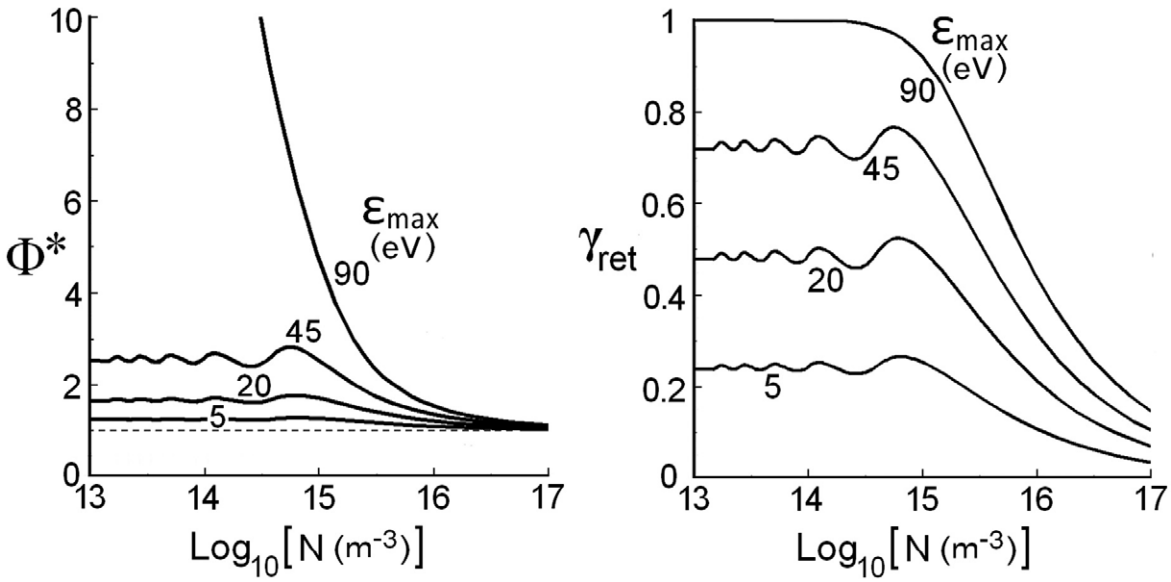

Figure 2. Calculation of γ_{ret} and Φ with varying ε_{max} and N. We plotted the normalized sheath potential $\Phi^* \equiv \Phi/\Phi_0$. The dotted line $\Phi^* = 1$ represents the predicted inverse sheath potential when amplification is neglected.

$$\Phi = \frac{T_{emit}}{q_e} \ln\left(\frac{\gamma_p - \gamma_{ret}}{1 - \gamma_{ret}}\right). \quad (5)$$

We assumed that $\gamma_p > 1$. Assuming that $\gamma_{ret} < 1$ (to be proven later), it follows that Φ increases with γ_{ret}. This is intuitive because when the emission self-amplifies, a larger fraction of it must be returned by the barrier for the wall to float. The value of γ_{ret} depends on the impact energies of the returning electrons and the wall's secondary emission yield. The parameter $\varepsilon_{max} \equiv 2m_e(E_z/B_x)^2$ is the maximum energy an electron can gain while drifting in an E × B field. So ε_{max} is the maximum energy a returning electron could gain parallel to the wall before impact. In systems where $\varepsilon_{max} < \sim 1$ eV, any drift motion is insignificant. Returning electron impact energies equal their emission energies $\sim T_{emit}$ (a few eV). No amplification occurs because such low energy electrons cannot knock out 'true secondaries' from solids [17].

The regime of interest here is where ε_{max} well exceeds a few eV, so that returning electrons could gain enough energy to eject true secondaries efficiently. In this regime, the initial parallel energy $\sim T_{emit}$ is small compared to ε_{max}, so the returning electron motion parallel to the wall resembles an electron starting from rest in an E × B field. The impact energy ε_{ret} depends on the time it takes to return to the wall τ_{ret},

$$\varepsilon_{ret}(\tau_{ret}) = \frac{\varepsilon_{max}}{2}\left[1 - \cos\left(\frac{B_x q_e}{m_e}\tau_{ret}\right)\right]. \quad (6)$$

The τ_{ret} for each secondary depends on its initial velocity $v_{x,emit}$ *normal* to the wall and the potential profile $\varphi(x)$. Calculating τ_{ret} exactly would require the exact numerical solution to Poisson's equation for $\varphi(x)$. So for the purposes of analytical estimation, we approximate that the inverse sheath's potential gradient is uniform, given by the average gradient $\Phi/\Delta x_{inv}$. The inverse sheath spatial width Δx_{inv} is estimated in [12] to be $(2\varepsilon_0\Phi/q_eN)^{1/2}$, where N is the interior plasma density. Each secondary thus faces deceleration $a = q_e\Phi/m_e\Delta x_{inv}$. The total return time is then $\tau_{ret} = 2v_{x,emit}/a = m_e v_{x,emit}(8\varepsilon_0/\Phi N q_e^3)^{1/2}$.

Now γ_{ret} is calculable in terms of the known secondary emission yield function $\gamma(\varepsilon)$ versus impact energy ε [17] for the wall material. Returning electrons with initial velocity $v_{x,emit}$ induce emission at the rate $\gamma(\varepsilon_{ret}(\tau_{ret}(v_{x,emit})))$, where $\varepsilon_{ret}(\tau_{ret})$ is (6), and $\tau_{ret}(v_{x,emit})$ was derived above. The average number of secondaries induced by all returning electrons γ_{ret} is the average of $\gamma(\varepsilon_{ret}(\tau_{ret}(v_{x,emit})))$ over the Maxwellian $v_{x,emit}$ distribution,

$$\gamma_{ret} = A^{-1}\int_0^{\sqrt{\frac{2q_e\Phi}{m_e}}} \exp\left(\frac{-m_e v_{x,emit}^2}{2T_{emit}}\right) \times\gamma\left[\frac{\varepsilon_{max}}{2}\left(1 - \cos\left(v_{x,emit}\sqrt{\frac{8B_x^2\varepsilon_0}{q_e\Phi N}}\right)\right)\right] dv_{x,emit}. \quad (7)$$

The upper integration limit $(2q_e\Phi/m_e)^{1/2}$ is the cutoff velocity separating returning secondaries from secondaries that escape to the plasma. The constant A is the normalization, given by the same integral without the 'γ[]' part. Because equation (7) contains Φ, it is coupled to equation (5) which contains γ_{ret}. Solving the equations numerically gives γ_{ret} and Φ in terms of known system properties.

2.2. Model predictions

In figure 2, γ_{ret} and Φ are plotted over a range of plasma properties. With B_x fixed at 0.01 T, we considered ε_{max} values of 5, 20, 45 and 90 eV. This corresponds to varying E_z between values of 67, 134, 201 and 282 V cm^{-1}. Typical values 2 eV for T_{emit} [17] and 1.5 for γ_p were chosen. To compute γ_{ret}, the function $\gamma_{BNC}(\varepsilon) = 0.17\varepsilon^{1/2}$ is used in (7) as a good fit to a common plasma-facing material boron nitride ceramics (BNC) [18] in the energy range of interest (up to a few hundred eV). The sheath

potential for this system would be $\Phi_0 \equiv T_{\rm emit}\ln(\gamma_p)/q_e = 0.81\,{\rm V}$ by (5) if there were no amplification. The plotted sheath potential in figure 2 is normalized to Φ_0 to emphasize the amplification.

In most sheath theories the sheath potentials are independent of plasma density N [9–12] because the fluxes of plasma electrons, ions and plasma-induced secondaries are all proportional to N. But figure 2 predicts that N has a strong influence on Φ. This surprising behavior here is due to a coupling between N and $\gamma_{\rm ret}$. Basically, when N is large, return times are too short for returning electrons to gain energy accelerating in E_z, so $\gamma_{\rm ret} \approx 0$. As N drops, the sheath's *width* $\Delta x_{\rm inv}$ increases. This reduces the potential gradient $\Phi/\Delta x_{\rm inv}$ responsible for returning the electrons, thereby increasing their return times, making $\gamma_{\rm ret}$ increase. Eventually $\gamma_{\rm ret}$ reaches a maximum and decreases when many returning electrons have time to complete more than a half gyration in the E × B drift, making their energies smaller. For further decreases of N, $\gamma_{\rm ret}$ exhibits a damped oscillation and converges to a limit when returned electrons with different $v_{x,\rm emit}$ are well phase mixed. The damped oscillations are present for the $\varepsilon_{\rm max}$ = 5, 20 and 45 curves in figure 2.

Beyond a critical $\varepsilon_{\rm max}$, a fundamentally different regime of behavior appears. It was intuitive that $\gamma_{\rm ret}$ would increase with $\varepsilon_{\rm max}$ in figure 2 (at fixed N) because returning electrons gain more drift energy when $\varepsilon_{\rm max}$ is larger. One might expect that $\gamma_{\rm ret}$ should increase beyond unity at high $\varepsilon_{\rm max}$ because many secondary yield functions including BNC's exceed unity at 10s of eV energies [17]. A $\gamma_{\rm ret}$ exceeding unity could lead to a destructive runaway generation of secondaries similar to a multipactor [19]. Instead, as $\gamma_{\rm ret}$ nears unity, Φ increases rapidly via (5). The increase of Φ helps limit return times in (7), preventing $\gamma_{\rm ret}$ from getting larger. So when $\varepsilon_{\rm max}$ is large, $\gamma_{\rm ret}$ approaches unity monotonically as N decreases, and Φ blows up, rather than converge. This explains the $\varepsilon_{\rm max}$ = 90 eV curves in figure 2.

The main physical factors behind returning electron dynamics and their amplification was captured in our discussion of figure 2 by varying E_z and N. Other parameters including B_x, $T_{\rm emit}$ and γ_p were kept constant. Varying these would affect $\gamma_{\rm ret}$ but will not lead to new physical phenomena. Varying B_x is equivalent to varying E_z and N because the parameters appear as ratios E_z/B_x and $B_x/N^{1/2}$ in equation (7). Increasing γ_p could increase or decrease $\gamma_{\rm ret}$ depending on the starting point in parameter space. Because the emission yield function $\gamma(\varepsilon)$ for most materials obeys a universal shape [17], using wall materials other than BNC will lead to qualitatively similar plots, with one caveat. Materials with low emission yields will never exhibit the 'blow up' amplification regime seen in the $\varepsilon_{\rm max}$ = 90 eV curve in figure 2. For example, if the material has $\gamma(\varepsilon) < 1$ for all ε, clearly $\gamma_{\rm ret}$ cannot approach unity regardless of the other system parameters.

The last parameter in the model is $T_{\rm emit}$. One might have expected from the beginning that because $T_{\rm emit}$ is 'small' in practice, the returned electrons get sent back promptly without time to gain drift energy. However, plugging (5) into (7) and substituting $v^* \rightarrow v_{x,\rm emit}/(T_{\rm emit})^{1/2}$ shows that $\gamma_{\rm ret}$ is independent of $T_{\rm emit}$. Only Φ is affected by $T_{\rm emit}$.

Table 1. Simulation results for different plasma densities N. $R_{\rm trans}$ and $R_{\rm heat}$ describe the enhancements of the integrated cross-field current and wall heating, respectively, due to returning electrons.

N (m^{-3})	Φ (V)	γ_p	$\gamma_{\rm ret}$	$\lvert R_{\rm trans}\rvert$	$R_{\rm heat}$
10^{17}	0.8	1.22	0.20	0.03	0.02
10^{16}	1.2	1.25	0.49	0.2	0.1
10^{15}	5.9	1.42	0.84	4.7	1.1
10^{14}	24.3	1.71	0.94	30	4.4

3. Simulations

3.1. Overview of the simulations

We now simulate an E × B discharge with a realistic $\varepsilon_{\rm max}$ to investigate returning electron effects. A planar plasma with uniform E × B background fields bounded by BNC walls is simulated using the electrostatic direct implicit particle-in-cell code [20]. This 1D3V code approximates the plasma heating and plasma-wall interaction physics in a HT cross section [21]. Development of the simulation model was motivated by experiments that show as the discharge voltage is increased, enhanced transport and energy loss arise [5]. These problems are attributed to strong secondary emission. Some theories predict the sheaths are SCL [5]. Theories and simulations have also shown that inverse sheaths are possible [12, 13]. In either case, returning secondaries exist. But their contribution to transport and energy flux was not analyzed in past simulations with inverse or SCL sheaths [12, 13, 22, 23].

Here we run new simulations with E_z = 325 V cm^{-1} and B_x = 115 G, giving $\varepsilon_{\rm max}$ = 91 eV. These field magnitudes were measured along the median of the PPPL HT with BNC walls, see figure 9 of [5]. We set the background uniform neutral xenon density to 10^{18} m^{-3} and use a turbulent collision frequency $0.7 \times 10^6\,{\rm s}^{-1}$, as in [21]. The plasma width is 20 mm. Four simulations are run at plasma densities N from 10^{17} to 10^{14}m^{-3}. Results are presented in table 1 and figure 3.

3.2. Discussion of simulation results

Table 1 shows that the sheath potential Φ varies strongly with N even though all other system properties are fixed. This is consistent with returning electron amplification, as theorized earlier. To measure amplification, we tracked the average number of secondaries induced by returning electrons $\gamma_{\rm ret}$. The average number of secondaries induced induced by plasma electrons (coming in from beyond the sheath edge) is γ_p. Table 1 indicates that $\gamma_{\rm ret}$ approaches unity as N drops, driving Φ to much higher values. Although $\gamma_{\rm p}$ also increases at lower N, this is not the driving cause of the stronger sheaths but is an *effect* of plasma electrons gaining more energy accelerating in a stronger sheath.

Figure 3 shows the cross-B current density near the left wall. Because the current in a discharge increases proportionally to N if all else equal, the plotted currents are each normalized $J_z^*(x) \equiv J_z(x)/N$ to compare transport 'efficiency' at different N. The currents in figure 3 are essentially all from secondary electrons (transport from e–n and turbulent collisions is weak in comparison). For $N = 10^{17}$ m^{-3}, almost all transport is to the right of the sheath edge, from escaped secondaries.

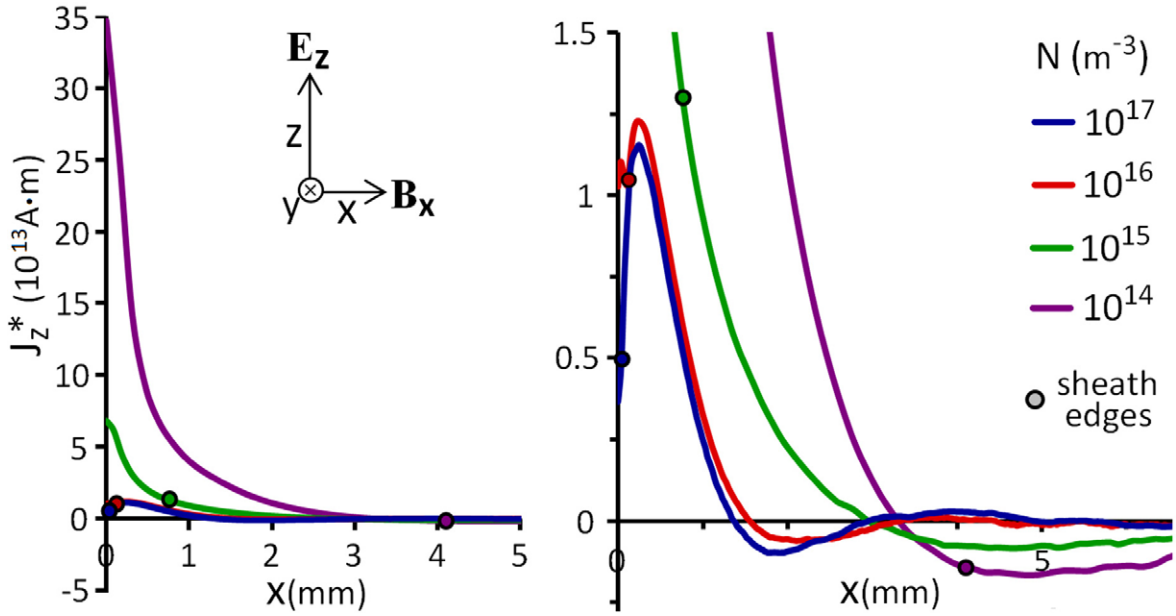

Figure 3. Normalized current density J_z/N versus distance from the left wall. To improve clarity, the plots are shown twice with different vertical scales. The location of the sheath edge in each run is marked on the corresponding curve.

Their 'NWC' oscillates in space and damps with distance due to phase mixing, as predicted by theoretical models [8], see figure 1(b). In the lower N runs, the emitted flux from the wall is much larger because γ_{ret} is larger. But the transport to the right of the sheath edge varies only modestly in magnitude because when an emission barrier is present, the flow of secondaries *escaping into the plasma* cannot get larger.

The new result here is that the returning electrons can also contribute NWC. The transport efficiency *inside the sheath* rises drastically as N drops, due to returning electrons amplifying to high intensities. We define $|R_{trans}|$ as the absolute ratio of the integrated cross-B current inside the sheath (from the wall to the sheath edge) to outside the sheath (from the edge to the midplane). We find that $|R_{trans}|$ increases from 0.03 to 30 as N drops from 10^{17} to 10^{14} m^{-3}. It must be noted that some of the cross-B current inside the sheath in each run is from secondaries that escape. However, the escaped secondaries cannot be responsible for the drastically increased cross-B current. Their NWC contribution is always zero at the wall [8] because secondaries start with zero *averaged* velocity perpendicular to **B**. Returning electron NWC generally has its maximum at the wall. So the transport efficiency growth at lower N in figure 3, which is strongest at the wall, is attributable to returning electrons.

The heating of the returning electrons in the E × B drift also adds to the heat flux deposited onto the wall. Table 1 lists R_{heat} in each run, defined as the ratio of heat flux from returning electron impacts to plasma electron impacts. We find that R_{heat} increases by a factor of 220 as N is reduced from $10^{17}m^{-3}$ to 10^{14} m^{-3}. The returning electron contribution to the total heat flux can vary from negligible to dominant.

3.3. Comparison between the theory and simulations

The theoretical model calculation of γ_{ret} in (5) and (7) was not intended to be exact, but it does a good job of predicting whether or not amplification is significant for a given set of conditions in the parameter space. The simulated field conditions are closest to the $\varepsilon_{max} = 90$ eV curves in figure 2. Based on the calculations in figure 2, one would predict amplification to be weak for $N \geq 10^{17}m^{-3}$, start becoming significant below $10^{16}m^{-3}$ and then blow up below $10^{15}m^{-3}$, as observed in Table 1. One source of error in calculating γ_{ret} is the linear approximation to $\varphi(x)$, which overestimates the τ_{ret} for some returning electrons and underestimates others. Also, the assumption that all secondaries have a single temperature T_{emit} is imprecise because there are always higher energy backscattered electrons [17] in addition to the true secondaries. The backscattered electrons become more significant in extreme amplification regimes where Φ exceeds a few T_{emit}. For example in the $N = 10^{14}m^{-3}$ run with $\Phi = 24.3$ V, all true secondaries with $T_{emit} = 2$ eV are returned and there is a large fraction of backscattered electrons in the returning electron population. The two species together modulate the amplification effect in a more complex way.

4. Implications

The possible importance of returning electrons was not previously considered to our knowledge. In E × B systems including HT's [15], Penning-type systems [24], magnetrons [25], transport is known to be dominated by anomalous mechanisms [5–7, 26] including fluctuations and NWC. Past theoretical models of NWC [8, 27] calculated transport from secondaries that enter a plasma (or from plasma electrons that reflect off sheath irregularities at a rough surface). Because the flow of these electrons into the plasma is limited by the maximum Γ_p, the NWC's contribution to an E × B discharge current is assumed to have a corresponding maximum, see the review of [5] and references therein. In particular, theoretical HT models [15, 28–30] assume the NWC

saturates at the SCL threshold. Similarly, predictions for energy flux to the walls in E × B systems [14] are based on sheath transmission equations [9] that count heat flow from bulk plasma electrons, which saturates at the SCL threshold. Overall, heat flux or NWC from returning electrons has not been considered.

The general implication of the current study is that the total NWC and energy flux can be larger than previously believed possible because the contribution of returning electrons is nonzero. Returning electrons could enhance transport, wall heating and global energy loss substantially under certain conditions, as shown by the theory and simulations. If present in experiments, amplification would feedback affect the properties of discharges in intricate ways that not demonstrated in the 1D simulations presented here where the background conditions were fixed.

For example, enhanced transport from secondary emission in Hall thrusters is known to feedback limit the achievable thrust field 'E_z' [5]. Many thrusters including the PPPL HT operate with high enough $\varepsilon_{\max}$ for amplification (10s of eV, inferred from measurements in the middle of the channel in figure 9 of [5]). The maximum distance along z that returning electrons can displace in their cycloidal motion $(2E_z m_e)/(q_e B_x^2)$ can be shown to be a few mm, short enough to guarantee that many returning secondaries are confined within the high E_z region. However, peak densities in the acceleration region are often $N > 10^{17}$ m^{-3}, where returning electron influence is predicted to be weak. We conclude that some amplification is probably present but is unlikely to play a major role compared to conventional NWC in high density thrusters. It should be noted that lower N plasmas are of interest for thrusters operating in pulsed mode [31] or with magnetically shielded surfaces [32]. Also, in any discharge, the plasma density starts out low during initial breakdown, so the presence of amplification could play a role on the discharge formation conditions. Therefore, future studies should further explore the possible presence of amplification effects in HT's and other E × B plasma systems.

5. Conclusions

5.1. Summary

Secondary electrons that return to plasma-facing walls in E × B systems drive a fundamental mechanism of energy flux and cross field transport not previously analyzed. If the returning electrons are heated by the E × B drift field enough that they eject secondaries upon impact, they will 'self-amplify'. If amplification is intense, the returning electron flux can exceed the flux of plasma electrons to the wall. Under these conditions, returning electrons may strongly influence the sheath amplitude, heating of the wall, cross field transport, and energy loss from the global system. We derived a theoretical model that can be used to predict the degree of amplification in terms of known properties of a system. Simulations of an E × B discharge with realistic fields confirmed that returning electrons are important in the range of conditions predicted by the theoretical model.

5.2. Other mechanisms of emission amplification

In this paper we considered amplification where secondaries induced by the plasma electrons return and knock out more secondaries. Amplification is also possible in principle at surfaces emitting 'strong' thermionic fluxes (equivalent to $\gamma_p > 1$). For example, in E × B discharges, the returning thermionic electrons collected by emissive probes could gain enough drift energy to induce *secondaries*, amplifying the same way. This would increase the probe heating and the probe's cross field current perturbation. However, because conductors tend to suppress electric fields from forming parallel to their surface, separate considerations of the parallel shielding effect are necessary to determine whether E_z is large enough anywhere in the sheath for amplification to occur at a metal surface. Photoemission can also provide 'seed electrons' for amplification. For example, Gascon *et al* pointed out that photoemission caused by xenon line radiation could significantly enhance the total emission from Hall thruster channel walls made of certain dielectrics including alumina [14]. Under the same range of system parameters where amplification of plasma-induced secondaries is predicted to be important, the returning photoelectrons may also induce secondaries.

Other mechanisms of emission amplification are possible in plasma systems where emitted electrons return to a surface with more energy than they started with. For instance, secondaries in tokamaks return to the divertor plates from gyration in the grazing **B** field (even if the sheath is classical) [33]. For flat plates, returning secondaries impact with only their initial energies by energy conservation within the sheath's **E** field. But divertor plates contain irregularities of various sizes, including Debye length scales [33]. In this regime one can envision that some secondaries which return to a more outward part of a surface irregularity can carry extra energy up to some fraction the classical sheath's (~100 V) mean potential. The extra energy could therefore be sufficient to induce more secondaries.

In systems where returning electrons gain no extra energy, they will impact with their initial emission energies ~T_{emit}, which is too low to eject secondaries. However, another 'amplification' mechanism might be relevant. Modern experiments show that backscattering probabilities are high at low impact energies for some materials [34, 35]. Repeated backscatters of the low energy returning electrons could then be possible at emitting surfaces under general conditions. For example, positively charged emitting dust grains collect returning electrons [2]. Charging dynamics would be significantly affected if the returning electrons backscattered multiple times before getting absorbed.

Acknowledgments

This work was supported in part by the US Air Force Office of Scientific Research, by the US Department of Energy under Contract No. DEAC02-09CH11466, and by the Walbridge Fund in the Princeton Environmental Institute at Princeton University.

References

[1] Ye M Y and Takamura S 2000 *Phys. Plasmas* **7** 3457
[2] Delzanno G L, Lapenta G and Rosenberg M 2004 *Phys. Rev. Lett*. **92** 035002
[3] Gunn J P 2012 *Plasma Phys. Control. Fusion* **54** 085007
[4] Ryutov D D 2005 *Fusion Sci. Technol*. **47** 148
[5] Raitses Y, Kaganovich I D, Khrabrov A, Sydorenko D, Fisch N J and Smolyakov A 2011 *IEEE Trans. Plasma Sci*. **39** 995
[6] Boeuf J P and Chaudhury B 2013 *Phys. Rev. Lett*. **111** 155005
[7] Smolyakov A I *et al* 2013 *Phys. Rev. Lett*. **111** 115002
[8] Morozov A I and Savel'ev V V 2001 *Plasma Phys. Rep*. **27** 570
[9] Hobbs G D and Wesson J A 1967 *Plasma Phys*. **9** 85
[10] Seon J, Lee E, Choe W and Lee H J 2012 *Curr. Appl. Phys*. **12** 663
[11] Sheehan J P *et al* 2013 *Phys. Rev. Lett*. **111** 075002
[12] Campanell M D 2013 *Phys. Rev.* E **88** 033103
[13] Taccogna F 2014 *Eur. Phys. J.* D **68** 199
[14] Gascon N, Dudeck M and Barral S 2003 *Phys. Plasmas* **10** 4123
[15] Meezan N B and Cappelli M A 2002 *Phys. Rev.* E **66** 036401
[16] Ordonez C A and Peterkin R E Jr 1996 *J. Appl. Phys*. **79** 2270
[17] Scholtz J J, Dijkkamp D and Schmitz R W A 1996 *Philips J. Res*. **50** 375
[18] Dunaevsky A, Raitses Y and Fisch N J 2003 *Phys. Plasmas* **10** 2574
[19] Kishek R A 2012 *Phys. Rev. Lett*. **108** 035003
[20] Sydorenko D 2006 *PhD Thesis* University of Saskatchewan
[21] Kaganovich I D *et al* 2007 *Phys. Plasmas* **14** 057104
[22] Sydorenko D *et al* 2009 *Phys. Rev. Lett*. **103** 145004
[23] Wang H *et al* 2014 *J. Phys. D: Appl. Phys*. **47** 405204
[24] Malmberg J H and Driscoll C F 1980 *Phys. Rev. Lett*. **44** 654
[25] Keidar M and Beilis I I 2006 *IEEE Trans. Plasma Sci*. **34** 804
[26] Taccogna F, Longo S, Capitelli M and Schneider R 2009 *Appl. Phys. Lett*. **94** 251502
[27] Barral S, Makowski K and Peradzyński Z *39th Joint Propulsion Conf.* (*Huntsville, AL, 2003*) AIAA paper 2003–4855
[28] Hara K *et al* 2014 *J. Appl. Phys*. **115** 203304
[29] Barral S *et al* 2003 *Phys. Plasmas* **10** 4137
[30] Ahedo E, Gallardo J M and Martinez-Sánchez M 2003 *Phys. Plasmas* **10** 3397
[31] Hruby V *et al* Hall thrusters operating in pulsed mode *27th Int. Electric Propulsion Conf.* (*Pasadena, CA, October 2001*)
[32] Mikellides I, Katz R R, Hofer D M, Goebel K, de Grys and Mathers A 2011 *Phys. Plasmas* **18** 033501
[33] Cohen R H *et al* 1999 *J. Nucl. Mater*. **266–9** 258
[34] Cimino R *et al* 2004 *Phys. Rev. Lett*. **93** 014801
[35] Schiesko L, Carrère M, Cartry G and Layet J-M 2008 *Phys. Plasmas* **15** 073507